A NOVEL OPTICAL TECHNIQUE FOR ACCURATE PLANAR MEASUREMENTS OF FILM-THICKNESS AND VELOCITY IN ANNULAR FLOWS

Charogiannis A., An J.S. and Markides C.N.*
*Author for correspondence
Clean Energy Processes (CEP) Laboratory,
Department of Chemical Engineering,
Imperial College London,
South Kensington Campus, London, SW7 2AZ,
United Kingdom,
E-mail: c.markides@imperial.ac.uk

ABSTRACT

Gas-liquid annular flow is one of many possible two-phase flow regimes that are encountered in the (e.g., parabolic collector) solar fields of direct-evaporation concentrated solar-power (CSP) plants. Conventional planar laser-induced fluorescence (PLIF) has been used previously to investigate the liquid film topology (i.e. film thickness) in annular flows, however, limitations have been found regarding the accurate identification of the gas-liquid interface with this technique, especially when the interface is smooth. Therefore, a novel variation of PLIF, which we refer to as structured planar laser-induced fluorescence (S-PLIF), has been developed to overcome these limitations. In this study, S-PLIF is used to investigate the topology of falling films in a vertical pipe over the range $Re_L \approx 150 - 1500$. Comparison of S-PLIF at two different angles (70° and 90°) shows that the technique performs better with an observation angle of 70° as this minimizes the distortions caused by the radial liquid film structure. In addition, S-PLIF70 shows good agreement with data from other techniques that have shown reliability when studying smooth films over the same range of conditions.

INTRODUCTION

Concentrated solar power (CSP) is a promising renewable-energy technology whose successful deployment relies crucially on effective performance improvements and cost reductions. CSP plants can employ either direct-steam generation or indirect/ secondary loops of heat-transfer oils or molten salts. Beyond the removal of a number of system components (intermediary heat exchangers, pumps, etc.), the former is considered advantageous due to the higher steam-temperatures that can be achieved, the reduced thermodynamic losses and higher efficiencies, and the reduced pumping losses at design-point operation. However, the (multiphase) fluid-flow and heat-transfer characteristics within the solar fields of such systems experience significant off-design or part-load unsteadiness due to the inherently time-varying environmental conditions (temperature, cloud coverage, diurnal irradiance), and employed flow-rates. Therefore, it is crucial to design these systems to operate effectively over different flow regimes, and over a range of varying heat-transfer characteristics, as may be encountered in practice.

NOMENCLATURE

ID	[m]	Internal diameter
L	[m]	Length
Q	[L/min]	Volumetric flow-rate
Re	[-]	Reynolds number
T	[°C]	Temperature

Special characters

δ	[mm]	Film thickness
θ	[°]	Angle
λ	[nm]	Wavelength
v	[m²/s]	Kinematic viscosity
ρ	[kg/m³]	Density
σ	[mm]	Film roughness
τ	[mm]	Laser sheet thickness

Subscripts

G	Gas
L	Liquid
PLIF	Planar laser-induced fluorescence
S-PLIF	Structured-PLIF

One type of two-phase flow regime that is encountered at high solar-fluxes and high flow-rates is the annular flow regime, which comprises a continuous thin liquid-film flow on the inner wall and a continuous gas core within the relevant collector fluid-conduits. In this flow regime, so-called 'ripple' and 'disturbance' waves are the two main types of interfacial waves that cover the surface of the liquid film. It is of great interest to identify and quantify these waves as they are associated with key phenomena such as liquid-droplet entrainment into the gas, and are thought to control the overall mass and heat transfer process in these flows. Generally, these flows are highly complex, 3-dimensional (3-D), and comprise moving and curved domains, all of which impose a significant challenge in the development of experimental techniques for their reliable characterization through accurate measurements of, e.g., the spatiotemporally varying liquid-film thickness.

Conventional planar laser-induced fluorescence (PLIF) has been used previously to investigate the spatiotemporal development of the liquid-film topology (i.e. film thickness) in annular flows [1,2,4-6]. The application of this technique, however, has limitations in identifying the gas-liquid interface when the films are smooth and the interface is flat, as total internal reflection of the emitted fluorescence results in

erroneous estimation of the local and instantaneous film thickness [2,3]. As an alternative to conventional PLIF, intensity/brightness-based laser-induced fluorescence (BBLIF), which does not suffer the same limitations when studying smooth films, has also been employed in similar studies. However, this technique is not without its own challenges; overestimation of the film thickness occurs whenever slopes are encountered, and underestimation can occur due to the presence of gas bubbles inside the liquid domain, such that this technique also becomes increasingly unreliable in progressively more complex flow regimes and locations. In both cases, solutions and corrections can be proposed to overcome these issues.

The present work focuses on improving conventional PLIF, mainly because BBLIF is less readily combined with standard techniques for the simultaneous measurement of the velocity field the flows of interest, for example by application of particle image velocimetry (PIV). This arises from the measurement principle on which BBLIF relies, according to which as the Lambert-Beer law is used to relate the local and instantaneous film thickness to the integrated fluorescence intensity in a line-of-sight in the film-height direction, which also means that the excited region of the flow is not visualized directly.

In this study, we propose a variation of the conventional PLIF technique, which we refer to as structured planar laser-induced fluorescence (S-PLIF), in order to accurately locate the gas-liquid interface in gas-liquid annular flows. In order to assess the efficacy of the proposed technique, film thickness data obtained by the application of S-PLIF are compared to data obtained by BBLIF and PLIF in the same flows.

FLOW FACILITY

Falling liquid-films were generated in the Downwards Annular Flow Laser Observational Facility (DAFLOF). A schematic of the flow facility is provided in Figure 1. The working fluid was deionized water, which was seeded with Rhodamine 6G dye at a concentration of approximately 4 mg/L. The liquid was circulated in a closed flow-loop with a variable speed vertical multi-stage centrifugal pump (CRiE3-15, Grundfos).

A turbine flow-meter (F110-X LCD, Fluidwell) was used to measure the liquid flow-rate, which was set to be in the range 3 – 9 L/min, whereas a Coriolis mass flow-controller (M15-AGD-22-0-S, Bronkhorst) was used when the imposed flow-rate was below 3 L/min. The water flowed through a conical injector at the top of the test section, thereby producing circumferentially uniform liquid-films on the pipe walls [7]. A refractive index matching approach was applied in the design of the test section which comprised a single FEP pipe with an internal diameter of 32.4 mm and a length of approximately 5 m, enclosed in a series of Perspex optical correction boxes, each measuring 70 mm × 60 mm × 1.3 m. The boxes allowed the pipe to be surrounded by deionized water, thus minimizing optical distortions caused by the curvature of the pipe, as is standard practice in these types of measurements.
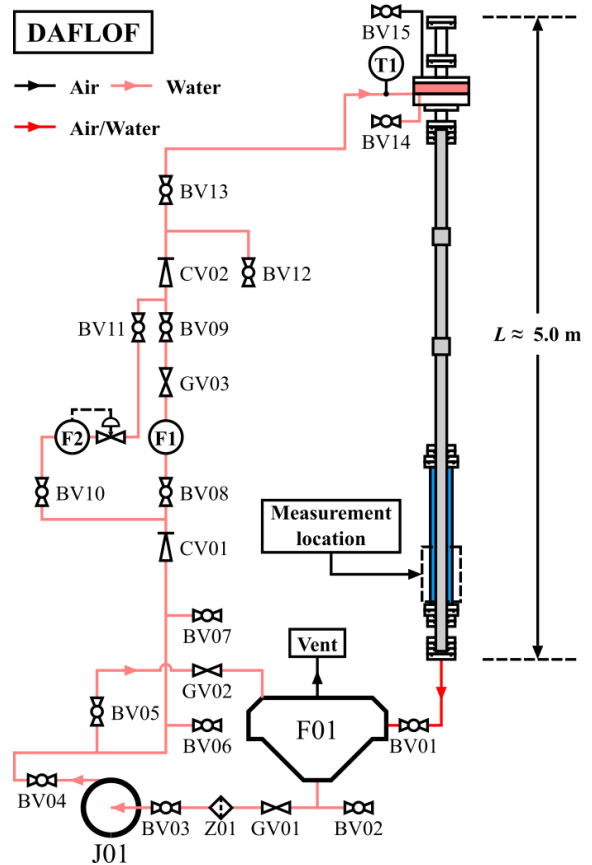
Figure 1 Schematic illustration of the DAFLOF

Optical measurements were conducted at a distance of 125 L/D (or, 4.0 m) downstream of the liquid injector in liquid falling-films over the Reynolds-number range Re_L = 147 − 1424 (see Table 1), and the temperature of the water during the experimental runs was 21.5 ± 1 °C. The definition of the liquid Reynolds number, Re_L is based here on the bulk-mean film velocity and the mean film thickness, $Re_L = (Q_L/\pi D^2)D/\nu_L$ [5].

Table 1 Examined flow conditions

| Q_L L/min	Re_L −
8.27	1424
7.45	1289
6.64	1153
5.84	1018
5.04	881
4.10	721
3.20	565
2.43	433
1.66	296
1.25	222
0.83	147

EXPERIMENTAL TECHNIQUE: S-PLIF

The optical arrangement used for the S-PLIF measurements is presented in Figure 2. A Ronchi ruling plate (5 l/mm, Edmund Optics) was positioned at the surface of the Perspex box, and a laser sheet (λ = 532 nm, $\tau \approx$ 200 µm) was sent through the plate at an angle of 30° to the horizontal. The laser sheet, which was

generated using a double-cavity frequency-doubled Nd:YAG laser (Nano-L-50-100PV, Litron Lasers) and dedicated laser-sheet optics, illuminated a longitudinal 2-D plane of the flow.

Images of the emitted fluorescence were collected using two CMOS cameras (VC-Imager Pro HS 500, LaVision) that were positioned at angles 70° and 90° relative to the excitation plane, in order to assess the effect of the camera observation angle on the resulting S-PLIF images. Conventional PLIF measurements were also performed, simultaneously to the S-PLIF measurements, for comparison purposes. Each camera was equipped with a Sigma 105 mm f/2.8 macro lens and a 540 nm long-pass optical filter. The measurement system was synchronized using a LaVision high-speed controller (HSC), and operated at $f = 100$ Hz using the LaVision DaVis software.

Prior to conducting the S-PLIF measurements, two preparatory steps were taken and later utilized in the processing of the S-PLIF images. The first step was the application of a graticule correction technique [1], which requires that a target is positioned at the excitation plane inside the test section and immersed in the working liquid. The target comprised a 2-D pattern of 1 mm × 1 mm crosses with a pitch of 2 mm. Images of the target were used to correct for perspective distortions in the raw S-PLIF images, and to determine the spatial resolution of the optical setup, which amounted to 27.4 µm. In the second step, the graticule was removed, the test section was flooded with the working fluid and excited with the structured beam. We refer to such images as reference images.
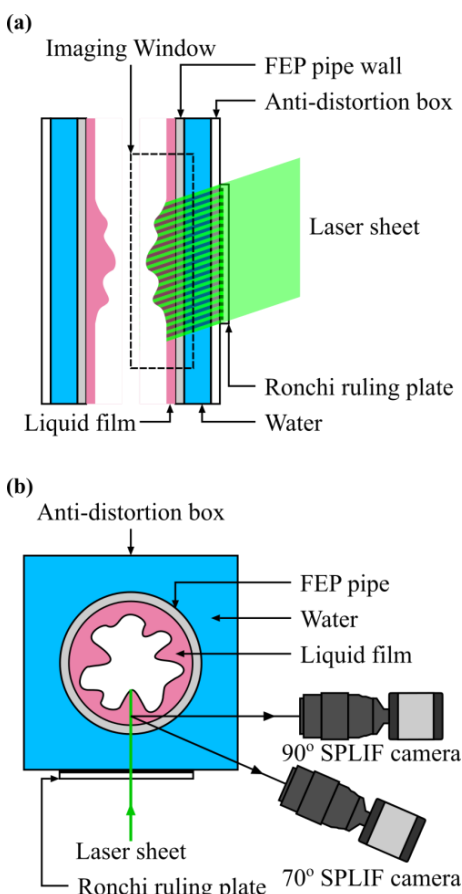
Figure 2 Optical S-PLIF arrangements: (a) side-, and (b) top-view

DATA PROCESSING AND RESULTS

One of the main challenges associated with the application of PLIF-based techniques is the development of reliable and robust processing routines that can be used to distinguish between the 'false' and the 'true' gas-liquid interfaces. For example, in the PLIF images presented by Zadrazil et al. (2014a) and later by Cherdantsev et al. (2016) who conducted PLIF and BBLIF measurements simultaneously, bright lines were occasionally observed within the emitted fluorescence, and were shown to coincide with the location of the true gas-liquid interface. Any fluorescence that was detected above these features was attributed to total internal reflection of the fluorescence emitted by the illuminated liquid bulk [2]. In another study, the presence of these reflections artefacts was shown to results in an overestimation of the mean film thickness of flat films by PLIF, by approximately 30% [3]. The aforementioned bright lines, however, could not be used to recover the location of the true gas-liquid interface consistently, as they were only occasionally available, and typically did not extend along the entire film domain.

A close examination of a raw S-PLIF image, such as the one shown in Figure 3(a), allows us to observe that the fluorescence signal comprises a pattern of lines due to the structured illumination. Of interest is the observation that the direction of these lines changes when the emitted fluorescence is reflected at the true gas-liquid interface, which forms the basis of our proposed technique. In order to render the change of direction of the lines more prominent, the laser sheet was inclined by 30° relative to the horizontal. MATLAB-based processing routines were developed in order to systematically identify the location of the gas-liquid interface, and comprised the following steps:

1. The raw S-PLIF images were corrected for perspective distortions based on the graticule images.
2. A 5 × 5 pixel median filter was applied to the corrected images. The intensity profile along each image column was then calculated and the filtered images were normalized by the maximum intensity.
3. The 2-D gradient magnitude and direction was determined for each normalized frame in order to produce frames such as the one shown in Figure 3(b) (which corresponds to the 2-D gradient direction frame).
4. Steps 1 − 3 were also applied to the reference image.
5. The 2-D gradient-direction frame of each S-PLIF image was subtracted from the reference image 2-D gradient-direction frame to give frames such as that in Figure 3(c).

Finally, the 'true' gas-liquid interface can be identified by setting a threshold value on the absolute difference between the two gradient-direction frames. Within the liquid domain, the absolute difference between the two gradient-direction frames gives near-zero values, while outside the liquid boundaries (including any regions that are plagued by total internal reflection), the absolute difference between the two gradient-directions frames is typically higher by 2 orders of magnitude.

The green lines in Figure 3(d), 3(e) and 4 represent the solid-liquid interface, the red lines represent the true gas-liquid interface recovered by S-PLIF, and the yellow lines represent the false gas-liquid interface recovered by PLIF. In all cases, the film is smoother and thinner when identified by S-PLIF

compared to PLIF, which is expected as the S-PLIF method discards the reflections about the gas-liquid interface [3]. It is also interesting to note that the deviations between PLIF and S-PLIF are smaller at certain locations along the film topology, such as the front slope of the disturbance wave shown in Figure 4(c). This can be attributed to the highly agitated interface at those locations, which suppresses the total internal reflection of the fluorescence emitted by the excited liquid film. The difference between the two methods can also be seen in Figure 5, where we plot the mean film-thickness $\langle \delta \rangle$ against Re_L.
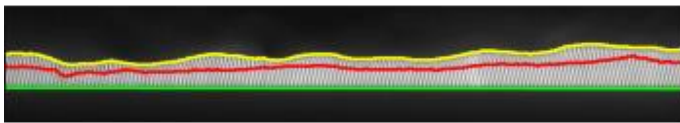
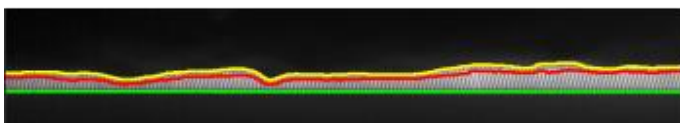**(a) Raw S-PLIF70 image**
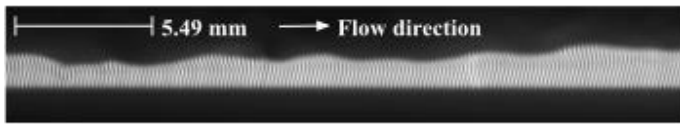
(b) 2-D gradient of image
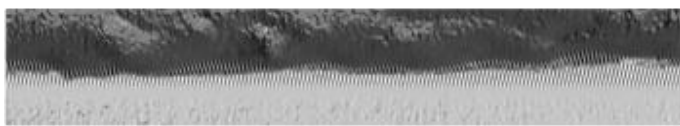
(c) Difference between reference image and S-PLIF image
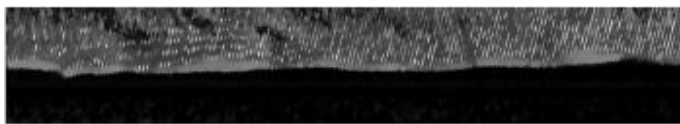
(d) Identified interfaces of S-PLIF70 image


(e) Identified interfaces of S-PLIF90 image

Figure 3 Processing steps shown on a falling-film image generated with $Re_L = 1505$: (a) raw image, (b) 2-D gradient, (c) difference, (d) identified interfaces for a S-PLIF70 image, (e) identified interfaces for a S-PLIF90 image.
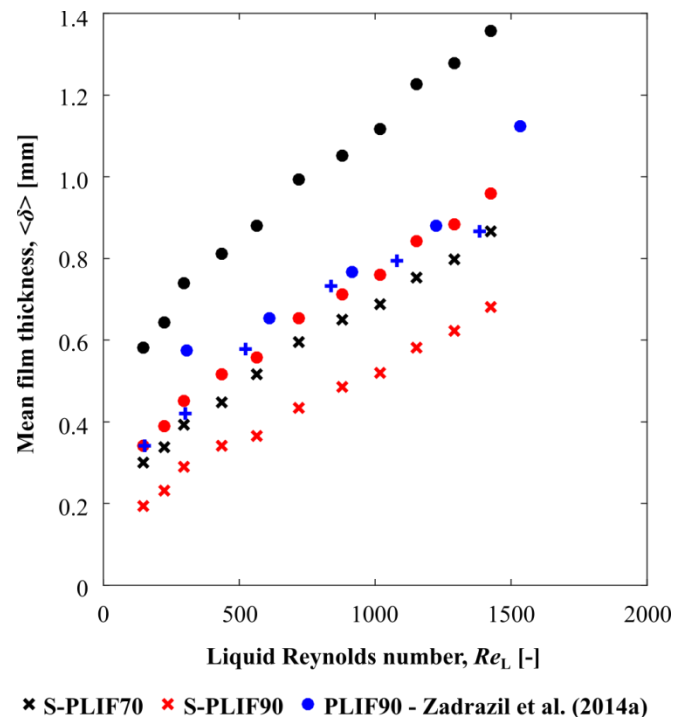
If we compare the data obtained based from the 70° and 90° S-PLIF (S-PLIF70 and S-PLIF90) configurations, referring to the arrangement used for the collection optics, there is a clear discrepancy in the identified location of the gas-liquid interface and, hence, of the film thickness. This is attributed to the local underestimation of the film thickness in the 90° measurement due to the transverse curvature of the liquid film [2], which can lead to the upper region of the film being 'hidden' to the camera. The effect of the transverse curvature decreases when setting the observation angle to 70° and the upper region of the film is more consistently exposed.

This same effect has been observed in the context of conventional PLIF, favouring PLIF70 in this regard. However, at 70° the spatial extent of the reflected fluorescence regions in PLIF is known to be larger than for the 90° case, which results in a larger deviation between the true and false interfaces and a greater overestimation of the film thickness by PLIF70. As we can see in this figure, the mean film thickness from PLIF70, is greater than that from S-PLIF70 by almost a factor of 2.

**Raw S-PLIF70 images at $Re_G = 0$ and $Re_L = 1505$**
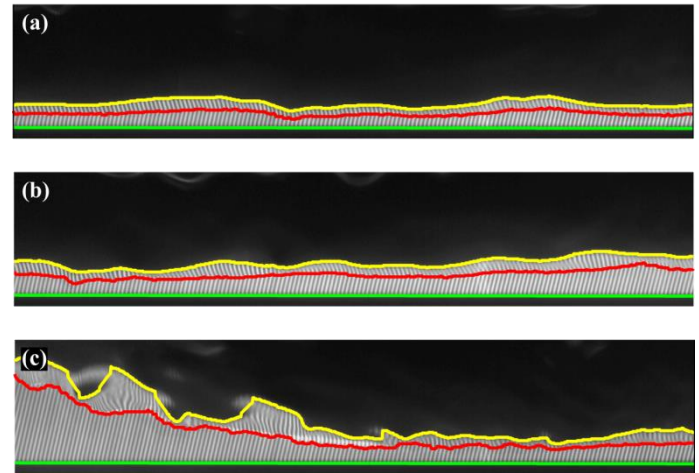
Figure 4 Fluorescence images showing the location of the two interfaces as determined by PLIF (yellow-lines) and S-PLIF (red-lines) methods, for a flow with $Re_L = 1505$.

× S-PLIF70   × S-PLIF90   ● PLIF90 - Zadrazil et al. (2014a)

● PLIF70   ● PLIF90   + BBLIF - Cherdantsev et al. (2016)

Figure 5 Plot of mean film-thickness, $\langle \delta \rangle$, against liquid Reynolds number, Re_L, from various falling-film measurements in the literature and from the present methods.

Even though, in general, local and instantaneous film thickness measurements recovered by the application of BBLIF and PLIF can vary significantly [2], the BBLIF-based mean film thickness data by Cherdantsev et al. (2016), the PLIF data by Zadrazil et al. (2014a), and our PLIF90 and S-PLIF70 data match closely (see Figure 5). It is interesting to note, therefore, that in our PLIF90 data and the PLIF data by Zadrazil et al. (2014a), any local overestimation due to the reflected interface is compensated by local underestimations due to the transverse curvature (3-D nature) of the interface when averaging in order to obtain the average film thickness.

Finally, in Figure 6, we present a scatter plot of local and instantaneous PLIF90 film-thickness data, $\delta_{PLIF90}(x,t)$, against corresponding S-PLIF70 film-thickness data, $\delta_{S\text{-}PLIF70}(x,t)$, from the same location and instant in the flow with $Re_L = 1505$. The red-line in this figure represents $\delta_{PLIF90} = \delta_{S\text{-}PLIF70}$. Here it can be seen that, thanks to aforementioned compensation of local overestimations from interface reflections by underestimations from the transverse interface curvature in the PLIF90 measurement, the resulting PLIF90 data in fact match the S-PLIF70 data for $\delta(x,t)$ to an acceptable level of accuracy (±5%), even in a local and instantaneous sense.
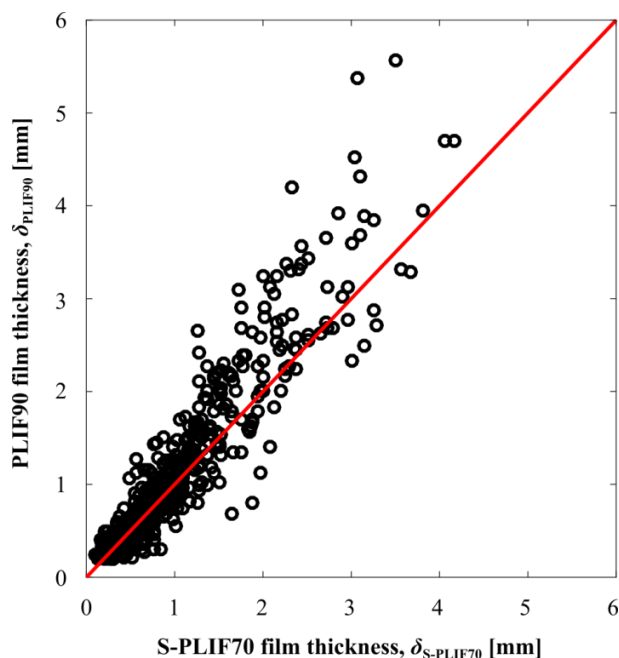
Figure 6 Scatter plot of PLIF90 film thicknesses, δ_{PLIF90}, against S-PLIF70 film thicknesses, $\delta_{S\text{-}PLIF70}$, for $Re_L = 1505$.

CONCLUSIONS

A novel PLIF technique, termed structured planar laser induced fluorescence (S-PLIF), was developed in order to overcome the limitations of conventional PLIF, when the latter is employed for the investigation of annular flows, especially in cases when the gas-liquid interface is smooth. Limitations include an overestimation of the local of film thicknesses due to total internal reflection and an underestimation of local film thicknesses caused by the transverse curvature (3-D nature) of the gas-liquid interface. In this study, two cameras were positioned at 70° and 90° to the excitation plane in order to evaluate the effect of the observation angle on the resulting S-PLIF and simultaneous conventional PLIF and film-thickness data. The techniques were applied to a range of falling-film pipe-flows, spanning a range of liquid Reynolds numbers of $Re_L = 150 - 1505$. A comparison of mean film-thickness data that were recovered by the applying the two techniques, showed that S-PLIF70 identified thinner and smoother films compared to PLIF, also in good agreement with intensity or brightness-based LIF data in the literature, which are known to be more reliable when the films are smooth and the interface is flat, over all investigated flow conditions The implementation of S-PLIF using a 70° observation angle was shown to be advantageous, as it prevented the loss of information that resulted when the observation angle was set to 90° due to fluorescence emission being refracted and reflected about the gas-liquid interface in the radial direction.

REFERENCES

[1] Charogiannis, A., An, J.S., and Markides, C.N., A simultaneous planar laser-induced fluorescence, particle image velocimetry and particle tracking velocimetry technique for the investigation of thin liquid-film flows, Experimental Thermal and Fluid Science, vol. 68, 2015, pp. 516-536

[2] Cherdantsev, A.V., An, J.S., Zadrazil, I. and Markides, C.N., An investigation of film wavy structure in annular flow using two simultaneous LIF approaches, Proceedings of the 12th International Conference on Heat Transfer, Fluid Mechanics and Thermodynamics, 11 – 13 July 2016, Spain

[3] Häber, T., Gebretsadik, M., Bockhorn, H., and Zarzalis, N., The effect of total reflection in PLIF imaging of annular thin films, International Journal of Multiphase Flow, vol. 76, 2015, pp. 64-72

[4] Schubring D., Ashwood, A.C., Shedd, T.A., and Hurlburt, E.T., Planar laser-induced fluorescence (PLIF) measurements of liquid film thickness in annular flow. Part I: Methods and data, International Journal of Multiphase Flow, vol. 36, 2010, pp. 815–824

[5] Zadrazil, I., Matar, O.K., and Markides, C.N., An experimental characterization of downwards gas–liquid annular flow by laser-induced fluorescence: Flow regimes and film statistics, International Journal of Multiphase Flow, vol. 60, 2014, pp. 87-102

[6] Zadrazil, I., and Markides, C.N., An experimental characterization of liquid films in downwards co-current gas–liquid annular flow by particle image and tracking velocimetry, International Journal of Multiphase Flow, vol. 67, 2014, pp. 42-53

[7] Zhao, Y., Markides, C.N., Matar, O.K., Hewitt, G.F., Disturbance wave development in two-phase gas–liquid upwards vertical annular flow. International Journal of Multiphase Flow, vol. 55, 2013, pp. 111–129